Structural properties, electronic structure, Fermi surface, and mechanical behavior of bcc Cr-Re alloys

N. I. Medvedeva,[1,2] Yu. N. Gornostyrev,[2,3] and A. J. Freeman[2]
[1]*Institute of Solid State Chemistry, Yekaterinburg, Russia*
[2]*Department of Physics and Astronomy, Northwestern University, Evanston, Illinois 60208-3112*
[3]*Institute of Metal Physics, Yekaterinburg, Russia*

(Received 16 July 2002; revised manuscript received 23 December 2002; published 8 April 2003)

The electronic structure and ground-state properties (lattice parameter, cohesive energy, bulk and tetragonal shear moduli) were calculated for bcc Cr and Cr-Re alloys over a wide range of Re concentration by the full-potential linear muffin-tin orbital method (FLMTO) with generalized gradient approximation (GGA). We show that the GGA predicts the commensurate antiferromagnetic Cr state as a ground state for the experimental volume with a small lower energy compared with the nonmagnetic state, but gives a large moment of $0.92\mu_B$. In the Cr-Re system the magnetism becomes weak with Re concentration and for 25% Re the mean Cr moment is about $0.05\mu_B$. Examining the Fermi surface of Cr-Re alloys within the modified rigid-band approximation, the electronic topological transition (ETT) is found to occur for 6% Re. A weakening of the Cr-Cr bonds near this ETT is considered as a possible microscopic reason for the ''small'' rhenium effect—the ductility enhancement in Cr(Mo,W)-Re alloys with small Re additions. As the mechanism for the ''large'' rhenium effect (near 25–35% Re) the formation of Cr-Re close-packed particles should play an important role together with the significantly weakened Cr-Cr bonding.

DOI: 10.1103/PhysRevB.67.134204 PACS number(s): 61.82.Bg, 62.20.Fe, 71.15.Nc

I. INTRODUCTION

Alloys based on the VIA group refractory bcc metals (Cr, Mo, W) are attractive materials for high-temperature applications. Among them, chromium alloys have advantages due to low density, high creep, and oxidation resistance.[1] Unfortunately, this potential has not been realized because of their room-temperature brittleness, which is a common feature of VIA metals. A significant improvement in the mechanical properties of those metals (both strength and plasticity) is caused by rhenium alloying with a concentration close to the solubility limit, the so-called rhenium effect.[1–6] In particular, the ductile to brittle transition temperature was lowered to $-196\,^{\circ}$C for the Cr+35 at.% Re alloy, compared with $150\,^{\circ}$C for recrystallized unalloyed Cr.[1,4]

In addition, a small increase in the plasticity of VIA metals was found for Re addition of about 5–6 at.% (''small'' rhenium effect), which is accompanied by some lowering of the yield stress—in contrast to the rhenium effect at large concentrations (''large'' rhenium effect). A number of possible mechanisms for the explanation of a ''large'' Re effect has been discussed.[1,3–11] Our recent calculations[11] support the view[7–9] that the formation of close-packed particles (CPP) plays an important role in the hardening effect of bcc refractory metals; it allows one to explain the increase of impurity solubility and may be considered as a possible reason for the Re effect at large concentrations.

Electronic structure calculations for Mo-Re alloys[13] demonstrated that a drastic change in the Fermi-surface topology, called an electronic topological transition (ETT), occurs at 6 at.% Re, which can be accompanied by peculiarities in thermodynamic potential derivatives that give rise to anomalies in thermodynamic and kinetic characteristics. It is known[14] in some cases that an ETT causes considerable phonon softening and may even lead to an isostructural phase transition. According to Refs. 12, 15, and 16, an ETT may point to a region of nonmonotonic variation in elastic constants, resulting in anomalous behavior of mechanical properties. Indeed, unusual behavior of the physical properties (thermopower, x-ray photoelectron spectra, mean-square atomic displacements, and deviation from Vegard's law) was found in Mo,[17,18] W,[19] and Cr (Ref. 20) alloys with 5–10 at.% Re. The experimental investigation of Cr-Re alloys demonstrated some peculiarities in the concentration dependencies of the Young and shear moduli at about 5 at.% Re.[20] However, the variation in the elastic constants obtained both for Cr-Re (Ref. 20) and W-Re alloys[12] was found to be too small for this Re concentration to explain the observed increase in plasticity; further, calculations for Mo-Re alloys[13] revealed no anomalies in the bulk modulus. Therefore, the suggested connection between the observed anomalous physical properties, the microscopic mechanism of the small rhenium effect and the ETT near 5–6 at.% Re is still open for discussion.

Distinct from nonmagnetic W and Mo, bcc Cr is antiferromagnetic with an incommensurate (I) spin-density wave (SDW) and its origin is explained by the nesting of the Fermi surface.[21] The magnetic properties of Cr-Re alloys strongly depend on the Re concentration: for 0.78 at.% Re, the I-SDW transforms to a commensurate state. The Néel temperature of pure Cr is 311.5 K, but it increases to 600 K for Re concentrations up to 5% and decreases above 10 at.% Re; at around 16 at.%, it decreases sharply to 160 K.[22] The Cr phase containing more than 18 at.% Re is superconducting.[23] The magnetism in Cr-Re alloys has been the subject of a number of studies.[21–25] The elastic properties of Cr-Re alloys were found to be dependent on Re concentration, temperature, and magnetism.[24,26] However, magnetoelastic effects were intensively investigated only for concentrations close to

 ©2003 The American Physical Society

the triple point (Re content ~ 0.3at. %) in the magnetic phase diagram. No previous attempts have been made to investigate the electronic structure of Cr-Re alloys and to relate concentration changes with the properties of these alloys.

In this paper, we concentrate on the mechanism of rhenium effects and the detailed discussion of magnetic behavior of Cr-Re alloys is beyond the framework of this paper. We present the electronic structure, ground-state characteristics (lattice parameter, bulk and shear moduli, cohesive energies), and Fermi surfaces for bcc Cr and ordered Cr-Re alloys in a wide range of Re concentrations. Examining the features of the electronic structure and the Fermi surfaces we suggest that the weakening of Cr-Cr bonding plays an important role in the mechanism of rhenium effects.

II. GROUND-STATE CHARACTERISTICS OF Cr-Re ALLOYS

The electronic structure calculations were performed with the first-principles full-potential linear muffin-tin orbital (FLMTO) method[27] without any shape approximation to the potential and charge density. We used the generalized gradient approximation (GGA) with the 1996 Perdew (P96) ($\kappa = 0.804$) functional for the exchange-correlation potential.[28] The standard triple-kappa basis (-0.01, -1.0, and -2.3 Ry) and the angular momentum cutoff for the interstitial fitting $l_{max}=5$ and inside muffin-tin spheres $l_{max}=6$ were taken. The antiferromagnetic (AFM) phase of bcc Cr was considered with a commensurate wave vector with two Cr atoms per simple cubic cell (the total energies for the SDW and commensurate AFM state were assumed to be very close[29]). The alloying effect was investigated with a 16-atoms per cubic $(2\times2\times2)$ supercell, where the substitution of one, two or four Cr atoms by Re (with coordinates (0,0,0); (0,0,0), (1,1,1); (0,0,0), (1,1,0), (1,0,1), (0,1,1) allowed us to model the Re effect for $x=6.25\%$, 12.5%, and 25% concentrations, respectively. The supercell approach for modeling substitutional chromium alloys by ordered compounds was shown[30] to give similar results with the coherent-potential approximation (CPA) and virtual crystal approximation taking into account disorder effects. We employed 120 and 35 k points in the irreducible wedge of the Brillouin zone for the Cr and Cr-Re supercells, respectively. The muffin-tin radii were chosen to be 2.2 a.u. for both Cr and Re spheres.

The ground-state parameters for bcc Cr (equilibrium lattice parameter a, magnetic moment, bulk B and tetragonal shear C' moduli) obtained from the local-density approximation (LDA) and GGA calculations are shown in Table I together with experimental and other theoretical data. In accordance with previous investigations,[29,32–36] we found that the local-density approximation (for the LDA calculations we used the von Barth–Hedin potential) gave poor agreement of the Cr ground-state parameters with experiment (Table I); it overestimates the bulk modulus by about 30–40% and underestimates the lattice parameter by 3–5%.

Both our FLMTO and previous full-potential linearized augmented plane-wave[31] calculations[29,32] demonstrate that the GGA corrections substantially improve the values of the lattice parameter and bulk modulus for the nonmagnetic (NM) phase and especially the AFM phase. However, we obtained an overestimated magnetic moment for the Cr atom ($0.9\mu_B$) at the equilibrium lattice parameter. It should be noted that neither of the density-functional methods (LDA, GGA) allowed us to correctly obtain both the structural properties and the magnetic moment simultaneously: if LDA gave the true magnetic moment for the experimental volume, the GGA gave a true magnetic moment for the compressed unit cell. This discrepancy was attributed to the overestimation of the magnetism in bcc Cr by GGA (Ref. 29) and to remaining errors of the LDA-GGA.[32] In addition, the structural and magnetic characteristics may not be correctly described since the first-principles calculations were performed for a commensurate AFM state which is not the true experimental one for Cr.[37]

TABLE I. Equilibrium lattice parameter a (Å), bulk modulus B (Mbar), shear constant C' (Mbar), and magnetic moment M (μ_B) for bcc Cr. The experimental data are cited from Ref. 32.

		a	B	C'	M
Experiment		2.88	1.91	1.51	0.62
Previous calculations	AFM-LDA [a]	2.80	2.65		0.70
	AFM-GGA [b]	2.91			1.4
	NM-GGA [c]	2.85	2.83	1.69	
	AFM-GGA [c]	2.87	1.89	1.74	1.1
Present results	NM-LDA	2.80	3.03	1.76	
	NM-GGA	2.85	2.74	1.70	
	AFM-LDA	2.80	2.69		0.68
	AFM-GGA	2.87	1.87	1.64	0.92

[a]Reference 33.
[b]Reference 29.
[c]Reference 32.

Distinct from Ref. 37 (where the lowest energy state was found to be nonmagnetic) and Ref. 29 (where the ground state was obtained to be AFM only with the equilibrium lattice parameter larger than the experimental value), in our GGA calculations the total-energy versus volume curve for the AFM phase is lower than that for the NM phase for $V/V_0 \geqslant 0.96$ (Fig. 1). The minimum energy of the nonmagnetic phase occurs only at a slightly larger volume ($V/V_0 = 0.966$), where the energy of the AFM phase is smaller by 0.22 mRy/atom. It is important to stress that the magnetic moment at $V/V_0 = 0.966$ is equal to $0.5\mu_B$, which close to the value for the SDW. The energy difference between the two phases at their equilibrium volumes is 0.57 mRy/atom. This value is an order-of-magnitude smaller than that obtained in Ref. 29 (4.8 mRy/atom) but nevertheless exceeds the estimated energy lowering of the NM phase due to the formation of the I-SDW (0.11 mRy/atom).[38] Thus, the GGA-P96 functional correctly predicts the AFM state at the equilibrium volume, results in a smaller energy difference between the NM and commensurate AFM phases, but cannot describe the true magnetic moment. The detailed discussion of antiferromagnetism in Cr lies outside the scope of this paper and we turn to the consideration of the ground-state properties of Cr-Re alloys.

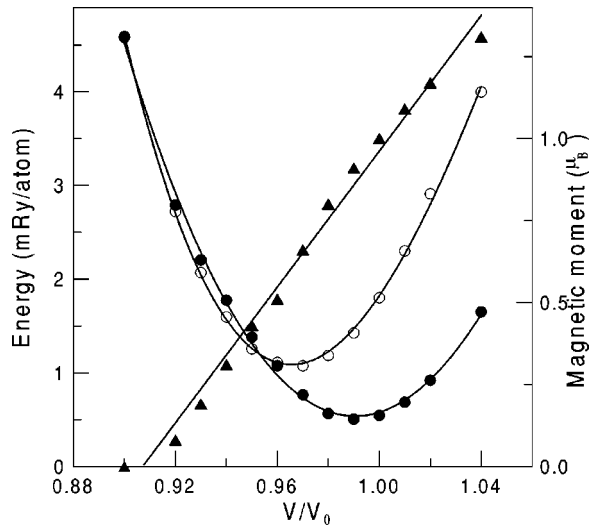

FIG. 1. (a) Total energy as a function of the volume ratio, V/V_0 (V_0 is the experimental volume) for nonmagnetic (open circles) and commensurate antiferromagnetic (solid circles) bcc Cr. Magnetic moment (triangles) as a function of volume V/V_0 for antiferromagnetic bcc Cr.

The concentration dependence of the structural characteristics obtained by the FLMTO-GGA calculations (Fig. 2) demonstrates the influence of magnetism on the elastic properties of Cr-Re alloys. The differences between the NM and AFM results are the largest for low Re content, decrease with Re concentration, and are absent for 25% Re. This behavior correlates with the Cr local magnetic moment (M); its mean values were calculated to be 0.48, 0.22, and $0.05\mu_B$, for 6.25%, 12.5%, and 25% Re, respectively. Thus, we found that the magnetism vanishes at about 25% Re and for the superconducting state ($x>18\%$) antiferromagnetism is strongly weakened ($M<0.1\mu_B$) in accordance with experimental results.[23]

The lattice parameter for the bcc Cr-Re alloys increases with the Re concentration for both the AFM and NM phases [Fig. 2(a)] and these linear dependencies are very close to the experimental data.[23] The opposite trend, namely, a decrease in the lattice parameter with Re concentration, was obtained for Mo-Re alloys within the linear muffin-tin orbital (LMTO) method.[13] The different behavior of the lattice parameter for these similar alloys may be understood from a comparison of the ionic radii, which are equal to 1.42, 1.55, and 1.52 Å for Cr, Mo, and Re,[39] respectively. Thus, an addition of Re to Mo results in a decrease in the lattice parameter, whereas for Cr alloys, the lattice parameter increases with Re additions.

We found for Cr alloys with $x>6\%$ Re that the bulk modulus B increases with Re concentration and is in good agreement with the experimental data obtained for paramagnetic Cr-Re alloys[26] (we extrapolated their experimental data to $T=0$). However, the bulk modulus for a small Re concentration decreases to its minimum near 6% both for the NM and AFM phases [Fig. 2(b)].

The difference between the elastic constants $C'=1/2(C_{11}-C_{12})$ [cf. Fig. 2(c)] characterizing tetragonal shear for the AFM and NM phases is much less than that for the bulk modulus. This agrees with the GGA results for bcc Cr (Ref. 32) and phenomenological theory[40] and demonstrates the smallness of the magnetic contribution to shear moduli. For both phases, a pronounced decrease of C' may be noted near 6% Re, and only small changes were found for larger Re concentration.

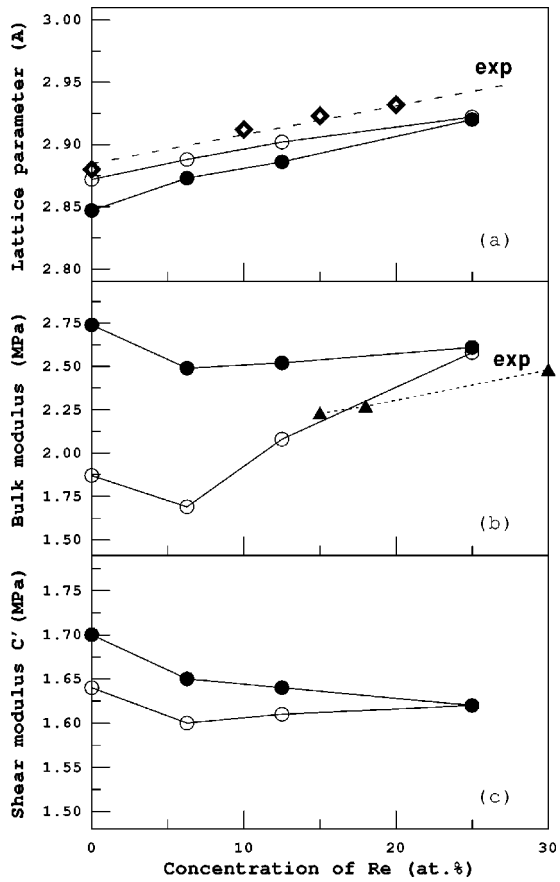

FIG. 2. (a) Lattice parameter, and (b) bulk and (c) shear moduli vs Re concentration for the NM (solid circles) and AFM (open circles) Cr-Re alloys. The open diamonds in (a) shows the experimental lattice parameters (Ref. 23) and the triangles in (b) show the experimental bulk modulus (Ref. 26).

III. ELECTRONIC STRUCTURE AND FERMI SURFACES OF bcc Cr-Re ALLOYS

Alloying with 6.25% Re leads [Fig. 3(a)] to a shift of E_F from a pronounced pseudogap in pure Cr onto a sharp slope, where the derivative of the density of states (DOS) has a singularity. A similar but weaker singularity in the DOS was found for the Mo-Re alloy with a Re concentration of about 6% (Ref. 13) and associated with the ETT.

The band structure and the Fermi surface (FS) of pure bcc Cr in the ΓNH plane of the Brillouin zone are shown in Figs. 4(a) and 4(b). The third d band forms the well-known octahedral and ellipsoidal hole pockets centered at points H and N of the bcc Brillouin zone, respectively. The fourth band gives an electron jack (distorted octahedron) with knobs centered at Γ and the fifth band gives small electron lenses along

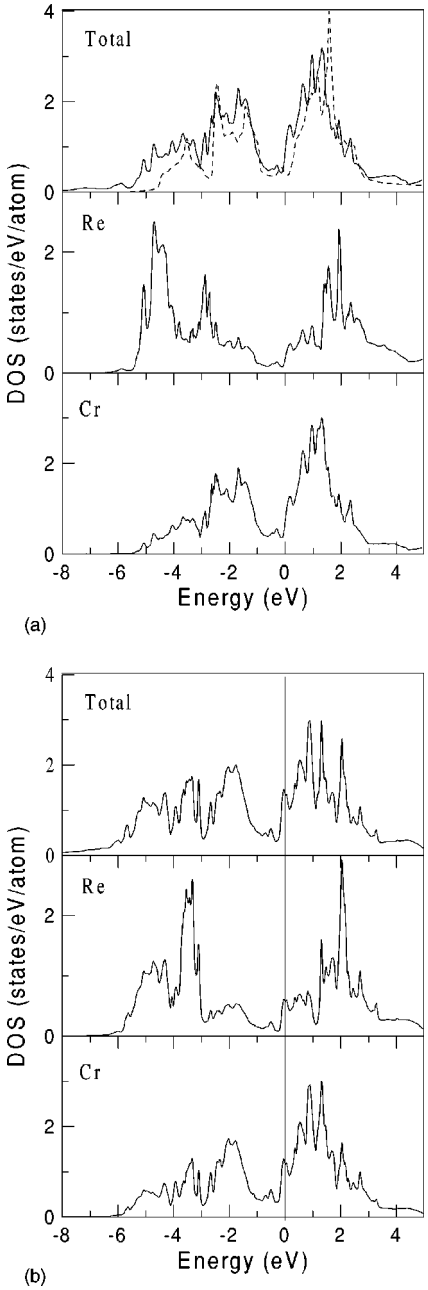

FIG. 3. Total and partial density of states (DOS) for (a) Cr +6.25% Re and (b) Cr+25% Re. The dashed line denotes the DOS for pure Cr. Energies are relative to the Fermi level, taken as zero.

Γ-H [Fig. 4(b)]. This FS topology for Cr is in a good agreement with that described previously[41,42] and is similar to the FS for bcc Mo.[13]

Proceeding to the consideration of the Fermi surface of Cr-Re it should be noted that a real FS calculation is problematic for the supercells consisting of a large number of nonequivalent atoms. The Fermi surface of the ordered intermetallic compound (supercell) used in our calculations for modeling Cr-Re alloys is quite different from that of disordered alloys due to additional band splitting. Therefore, to examine ordered alloys we used the rigid-band scheme for the discussion of possible changes in the Fermi surface with Re concentration. As regards the applicability of the rigid-band approach (RBA) we considered separately the effects of lattice variation (dilation) due to alloying and the additional electrons per Cr atom. The Cr FS calculated with the lattice constant corresponding to Cr+25% Re shows very small changes in the Γ-centered octahedron, slightly favoring the neck formation [dashed line in Fig. 4(b)].

The addition of extra electrons to Cr, up to a total of $24.1e$, keeps the Fermi level in the pseudogap, and a sharp increase of the Cr DOS similar to that in Fig. 3(a) (6% Re) occurs only at $24.25e$. It is seen from Fig. 3(a) that the DOS of pure Cr should be shifted by 0.23 eV to achieve a similar behavior near E_F with Cr+6% Re DOS. Indeed, as has been reported[43–45] the RBA is a rather good approximation for $E<E_F$, but the RBA DOS is shifted to higher energies for $E>E_F$. As a result new FS sheets are formed much faster than the RBA predicts. The failure of the simple RBA based only on an electron count seems to be the main reason for the discrepancy in Re concentration where the neck is predicted: 6% for the Mo-Re alloy within the CPA,[13] 20% for the W-Re alloy,[12] and 20–30% for the Cr-Mn alloy[43] within the RBA. For this reason we used a modified RBA combined with supercell calculations, in which the position of E_F was a parameter defined by comparison of the DOS for bcc Cr and the Cr+6%-Re supercell rather than by electronic count.

With increasing Re concentration, the Fermi energy rises; as a result the electron jack expands, the octahedral hole pockets are compressed, the ellipsoidal hole pockets become a bit smaller, and the electron lenses increase substantially. When E_F is shifted up at 0.23 eV, the electron jack touches the NH line; this means that the neck between the two electronic parts appears inside the Γ-N-H triangle [Fig. 4(c)]. As follows from the band structure [Fig. 4(a), see also Fig. 1 in Ref. 13), the ETT takes place when E_F intersects the fourth band along the NH. The FS topology in Fig. 4(b) is similar to that for the random alloy $Mo_{94}Re_{06}$ calculated within the LMTO-CPA.[13] It allows one to suggest that the neck in Cr-Re is formed at the same concentration (6% Re) as that in the Mo-Re alloys.

With increasing E_F, the process proceeds monotonically and the neck portion is expanded without any topological changes up to the shift of E_F at 0.7 eV. At this E_F, drastic changes occur in the FS [Fig. 4(d)]: (i) the electron jack is expanded greatly and there is a small gap between the H hole and the electron parts, (ii) the ellipsoidal hole N pockets disappear, and (iii) the electron lenses become so large that they join together and form a new sheet centered at Γ. These changes are connected with the occupation of the low-dispersion d band along N-Γ. Comparing the DOS for pure Cr and Cr+25% Re, one can assume that the second ETT corresponds to a higher Re concentration and most likely does not occur within the stability range of bcc Cr-Re alloys.

As mentioned in the Introduction, an ETT may influence the ground-state characteristics leading to anomalies in thermopower and kinetic and mechanical properties.[12,13,15–17,19,20] In the next section, we discuss the

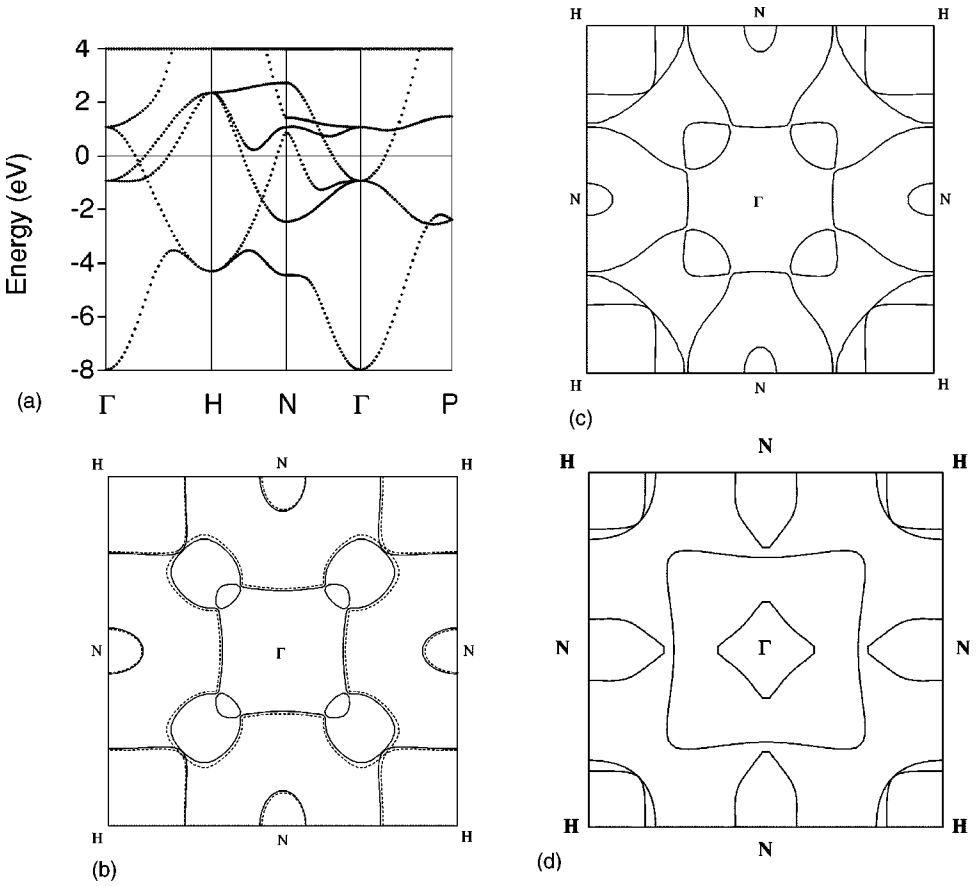

FIG. 4. (a) The band structure for bcc Cr and (b) sections of the Fermi surface for bcc Cr and (c) and (d) sections of the Fermi surface for Cr-Re alloys obtained in the rigid-band approximation for the shift of E_F by 0.23 eV and 0.70 eV, respectively.

possible relationship between the ETT and mechanical behavior.

IV. ELECTRONIC STRUCTURE PECULIARITIES AND THE RHENIUM EFFECT

Our calculated results reveal only small changes in the moduli for concentrations of about 6% Re, where the ETT takes place. No peculiarities in the concentration dependence of the bulk modulus (which gradually increases with Re) and heat capacity[46] were found in Mo-Re and W-Re alloys. The smearing due to disorder was considered[13] as an explanation of this fact. The absence of the peculiarities may also be explained by a weaker ETT effect on the electronic structure of Mo-Re compared with Cr-Re, which follows from a much weaker DOS singularity [the magnitude of the logarithimic derivative of the density of states, $d \ln N(E)/dE$, is 23 and 95 states/Ry for 5–6% Re in Mo[13] and in Cr, respectively]. Additionally, the opposite concentration dependencies of the lattice parameter in Cr-Re and Mo-Re alloys may influence the behavior of the bulk modulus. The chromium lattice expansion with Re concentration is a factor favoring a decrease in the bulk modulus, in contrast to Mo-Re alloys, where a decrease in volume makes for an increase in B with Re.

The bulk modulus increasing with Re concentration is a common feature of VI*a* metal alloys,[12,13,20,26] which points to a strengthening of chemical bonding by rhenium additions as witnessed by the cohesive energies which were estimated for nonmagnetic Cr-Re alloys to be 9.39, 9.66, 9.80, and 9.93 eV/atom for 0%, 6.25%, 12.5%, and 25% Re, respectively. On the other hand, a shift of E_F with Re concentration to higher energies leads to progressive filling of antibonding Cr states (Fig. 3) and, consequently, to a weakening of the Cr-Cr bonding. However, the occupation of antibonding states does not appear in the total bond strength, as follows from the concentration behavior of the cohesive energy which is an integral characteristic of interatomic interactions. It is seen from the charge densities (Fig. 5) that Cr-Re bonds appear with increased population, which compensates for the decrease in the Cr-Cr contribution to the cohesive properties due to the *d*-band filling effect and also to an increase in lattice parameter.[47]

The peculiarities of interatomic interactions and the connection between ETT and bond strength may be demonstrated based on the crystal orbital overlap populations (OP) curve obtained for the first and second-nearest-neighbor Cr atoms (Fig. 6) (a similar OP curve was reported in Ref. 47). The Fermi level in pure Cr falls in the pseudogap between bonding (positive OP) and antibonding (negative OP) states. For low Re concentrations, E_F remains in the pseudogap and a sharp increase both in the DOS and antibonding OP is

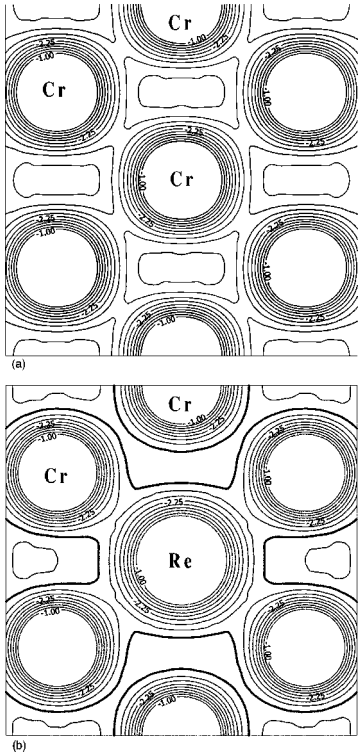

FIG. 5. The valence charge densities (in units of $e/\text{Å}^3$) for the {110} plane of (a) Cr and (b) Cr+6.25% Re.

observed only for an E_F shift at about 0.2 eV, corresponding to 5–6% Re. This correlates with the population of the fourth antibonding *d* band and the first ETT (the appearance of a neck along *NH*). An anomalous decrease of Cr-Cr bonding in Cr-Re alloys was suggested at about 5% Re based on the peculiarities of x-ray photoelectron spectra (minimum of intensity peak), the lattice parameter (maximum of the deviation of the lattice parameter from Vegard's law), and the mean-square atomic displacements.[20] The subsequent occupation of antibonding *d* states will lead to the progressive weakening of Cr-Cr bonding and to the instability of the bcc structure for high Re concentration. It is interesting to note

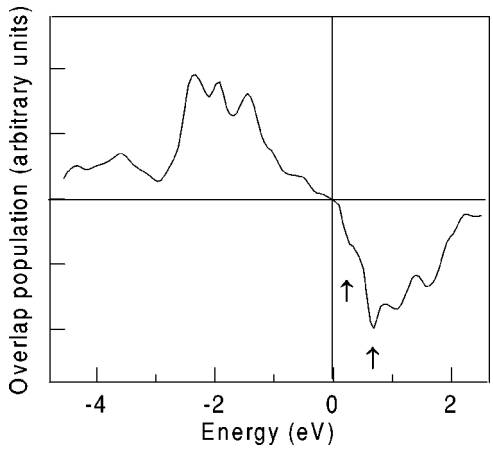

FIG. 6. Overlap population for bcc Cr obtained with the LMTO tight-binding method (Ref. 48) (only two nearest chromium atoms are included). The arrows correspond to the ETT's.

that the position of a deep minimum of the total Cr-Cr OP curve correlates with the second ETT.

Thus, the increase in electron concentration leads to a weakening of the bonding between the nearest Cr atoms. It should be mentioned that the decrease in Cr-Cr interatomic interactions takes place locally and so is not necessary to appear in overall cohesive characteristics such as bulk modulus and cohesive energy due to the compensating effect of rather strong Cr-Re bonds. The weakening of Cr-Cr bonds will decrease the energy barrier for the displacement of the atomic chain along the $\langle 111 \rangle$ direction in such a manner that a degenerate (hard) to nondegenerate (easy) dislocation core transformation should take place.[49] Since nondegenerate dislocations in the bcc lattice usually have a higher mobility in comparison with degenerate ones, it should be expected that the yield stress is lowered and the plasticity increased at the Re concentration corresponding to the first ETT. Thus, we conclude that the ''small'' rhenium effect is closely connected with the softening of Cr-Cr bonds near the ETT.

The sharp weakening of Cr-Cr bonding alone is not able to explain comprehensively the ''large'' rhenium effect when both the plasticity and strength increase simultaneously. The formation of close-packed particles (CPP) was suggested[7–9,11] as a possible mechanism for explaining this phenomenon. Indeed, in examining the calculated charge density in Fig. 5 we see a demonstration of the possible formation of Cr(Mo)-Re clusters with a rather strong charge density near Re. The A15-type structure was assumed for these CPP in Refs. 7 and 11. These precipitates may scavenge carbon impurities and prevent the formation of brittle carbides, whose appearance is considered to be one of the reasons for the chromium brittleness. Further, precipitation hardening is expected due to these clusters, which are obstacles for the motion of dislocations and will result in increased strength of Cr(Mo)-Re alloys.

V. SUMMARY

We presented first-principles calculations of the ground-state properties of bcc Cr and ordered Cr-Re alloys. Using the GGA-P96 functional, the commensurate antiferromagnetic phase of bcc Cr was found to be the lowest state with a rather small preferable energy below the nonmagnetic phase. The calculated lattice parameter and elastic moduli for AFM Cr were found to be in good agreement with previous calculations and experiment. The magnetism is weakened with Re addition and for 25% Re the local Cr magnetic moment is close to zero.

A small decrease in the moduli was found for concentrations of about 6% Re, where the ETT takes place, and the lattice expansion with Re concentration is considered as a factor favoring this decrease. The ETT is accompanied by a weakening of the Cr-Cr bonding between first and second neighbors. This is not revealed in the cohesive energy due to the compensating effect of Cr-Re bonds; however, it can lead to an increase in the dislocation mobility. Thus, a mechanism for the ''small'' rhenium effect may be understood in terms of the weakening of the Cr-Cr bonding and is closely connected with the first ETT. For the explanation of the ''large''

rhenium effect where both plasticity and strength are enhanced it is necessary to involve also the formation of close-packed Cr-Re particles that prevent the formation of brittle precipitates and lead to additional hardening. Since the electronic structure is very close for isoelectronic Cr, Mo, and W, this mechanism should be expected to be similar for all refractory bcc metals alloyed with rhenium.

ACKNOWLEDGMENTS

We thank D.L. Novikov for the help with the FLMTO calculations. Work at Northwestern University was supported by the Air Force Office of Scientific Research (Grant No. F49620-95-1-0189) and in part by the Russian Foundation for Basic Research (Grant No. 01-02-16108).

[1] W. D. Klopp, *Recent Developments in Chromium and Chromium alloys*, NASA Technical Report No. 70N20869, 1970 (unpublished).
[2] E. M. Savitskii, M. A. Tylkina, and K. B. Povarova, *Rhenium-based Alloys* (Nauka, Moskow, 1965), p. 335 (in Russian).
[3] V. I. Trefilov, Yu. V. Milman, and S. A Firstov, *Physical Background of the Strength of Refractory Metals* (Naukova Dumka, Kiev, 1975), p. 313 (in Russian).
[4] J. R. Stephens and W. D. Klopp, Trans. Soc. Min. Eng. AIME **242**, 1837 (1968).
[5] W. D. Klopp, J. Less-Common Met. **42**, 261 (1975).
[6] *Rhenium and Rhenium Alloys*, edited by Boris D. Bryskin (TMS, Warrendale, PA, 1997), pp. 629–728.
[7] Yu. N. Gornostyrev, M. I. Katsnelson, A. V. Trefilov, and R. F. Sabiryanov, Phys. Met. Metallogr. **74**, 421 (1992).
[8] Yu. N. Gornostyrev, M. I. Katsnelson, and A. V. Trefilov, in *Rhenium and Rhenium Alloys*, edited by Boris D. Bryskin (TMS, Warrendale, PA, 1997), p. 681.
[9] Yu. N. Gornostyrev, M. I. Katsnelson, and A. V. Trefilov, J. Phys.: Condens. Matter **9**, 7837 (1997).
[10] A. D. Korotaev, A. N. Tyumentsev, and Yu. I. Pochivalov, in *Rhenium and Rhenium Alloys*, edited by Boris D. Bryskin (TMS, Warrendale, PA, 1997), p. 661.
[11] N. I. Medvedeva, Yu. N. Gornostyrev, and A. J. Freeman, Acta Mater. **50**, 2457 (2002).
[12] Yu. N. Gornostyrev, M. I. Katsnelson, G. V. Peschanskikh, and A. V. Trefilov, Phys. Status Solidi B **164**, 185 (1991).
[13] N. V. Skorodumova, S. I. Simak, I. A. Abrikosov, B. Johansson, and Yu. Kh. Vekilov, Phys. Rev. B **57**, 14 673 (1998).
[14] M. I. Katsnelson, I. I. Naumov, and A. V. Trefilov, Phase Transitions **49**, 143 (1994).
[15] E. Bruno, B. Ginatempo, E. S. Giuliano, A. V. Ruban, and Y. K. Vekilov, Phys. Rep. **249**, 355 (1994).
[16] V. G. Vaks and A. V. Trefilov, J. Phys. F: Met. Phys. **18**, 213 (1988).
[17] A. N. Velikodnyi, N. Z. Zavaritskii, T. A. Ignat'eva, and A. A. Yurgens, Pis'ma Zh. Éksp. Teor. Fiz. **43**, 597 (1986) [JETP Lett. **43**, 773 (1986)].
[18] T. A. Ignat'eva and A. N. Velikodnyi, Low Temp. Phys. **28**, 403 (2002).
[19] K. B. Povarova, I. D. Marchukova, C. C. Budagovskii, and V. M. Koltygin, *Metal Monocrystals* (Nauka, Moscow, 1990), p. 213 (in Russian).
[20] O. A. Bannykh, I. D. Marchukova, and K. B. Povarova, Metalli. **3**, 49 (1997) [Russ. Metall. **3**, 43 (1977)].
[21] E. Fawcett, H. L. Alberts, V. Y. Galkin, D. R. Noakes, and J. V. Yakhmi, Rev. Mod. Phys. **66**, 25 (1994).
[22] A. L. Trego and A. R. Mackintosh, Phys. Rev. **166**, 495 (1968).
[23] Y. Nishihara, Y. Yamaguchi, T. Kohara, and M. Tokumoto, Phys. Rev. B **31**, 5775 (1985).
[24] A. H. Boshoff, H. L. Alberts, P. de V. du Plessis, and A. M. Venter, J. Phys.: Condens. Matter **5**, 5353 (1993).
[25] E. Fawcett, Physica B **239**, 71 (1997).
[26] H. L. Alberts, Physica B **161**, 87 (1989).
[27] M. Methfessel and M. Scheffler, Physica B **172**, 175 (1991).
[28] J. P. Perdew, S. Burke, and M. Ernzerhof, Phys. Rev. Lett. **77**, 3865 (1996).
[29] D. J. Singh and J. Ashkenazi, Phys. Rev. B **46**, 11 570 (1992).
[30] M. van Schifgaarde, F. Herman, S. S. P. Parkin, and J. Kudrnovsky, Phys. Rev. Lett. **74**, 4063 (1995).
[31] E. Wimmer, H. Krakauer, M. Weinert, and A. J. Freeman, Phys. Rev. B **24**, 864 (1981).
[32] G. Y. Guo and H. H. Wang, Phys. Rev. B **62**, 5136 (2000).
[33] J. Chen, D. Singh, and H. Krakauer, Phys. Rev. B **38**, 12 834 (1988).
[34] J.-H. Xu, A. J. Freeman, and T. Jarlborg, Phys. Rev. B **29**, 1250 (1984).
[35] A. T. Paxton, M. Methfessel, and H. M. Polatoglou, Phys. Rev. B **41**, 8127 (1990).
[36] G. Y. Guo, H. Ebert, W. M. Temmerman, K. Schwarz, and P. Blaha, Solid State Commun. **79**, 121 (1991).
[37] P. M. Marcus, S. L. Qiu, and V. L. Moruzzi, J. Phys.: Condens. Matter **10**, 6541 (1998).
[38] K. Hirai, J. Phys. Soc. Jpn. **66**, 560 (1997).
[39] W. A. Harrison, *Electronic Structure and the Properties of Solids* (Freeman, San Francisco, 1980).
[40] M. B. Walker, Phys. Rev. B **22**, 1338 (1980).
[41] S. B. Dugdale, H. M. Fretwell, D. C. R. Hedley, M. A. Alam, T. Jalborg, G. Santi, R. M. Singru, V. Sundararajan, and M. J. Cooper, J. Phys.: Condens. Matter **10**, 10 367 (1998).
[42] M. Biasini, Physica B **275**, 285 (2000).
[43] D. D. Koelling, Phys. Rev. B **59**, 6351 (1999).
[44] S. S. Rajput, R. Prasad, R. M. Singru, S. Kaprzyk, and A. Bansil, J. Phys.: Condens. Matter **8**, 2929 (1996).
[45] B. Kyung, Physica C **301**, 85 (1998).
[46] F. J. Morin and J. P. Maita, Phys. Rev. **129**, 1115 (1963).
[47] The cluster DVM-$X\alpha$ method [Y. Matsumoto, M. Morinaga, T. Nambu, and T. Sakaki, J. Phys.: Condens. Matter **8**, 3619 (1996)] also demonstrated an increase in the total bond order in Cr-Re alloys owing to stronger Cr-Re bonds.
[48] G. Krier, O. Jepsen, A. Burkhardt, and O. K. Andersen, TB-LMTO-ASA program, version 4.7 (Max-Planck Institute, Stuttgart, 1995).
[49] S. Takeuchi, Philos. Mag. A **39**, 661 (1979).